electronics

Review

MIMO Dielectric Resonator Antennas for 5G Applications: A Review

Hamza Ahmad [1], Mohd Haizal Jamaluddin [1,*], Fauziahanim Che Seman [2] and Muhibur Rahman [3,*]

[1] Wireless Communication Center, Faculty of Electrical Engineering, Universiti Teknologi Malaysia, Johor Bahru 81310, Malaysia; hamzaahmad@graduate.utm.my
[2] Faculti Kejuruteraan Elektrik dan Elektronik, Univeristi Tun Hussein Onn Malaysia, Parit Raja 86400, Malaysia; fauziahs@uthm.edu.my
[3] Department of Electrical Engineering, Polytechnique Montreal, Montreal, QC H3T 1J4, Canada
* Correspondence: haizal@fke.utm.my (M.H.J.); muhibur.rahman@polymtl.ca (M.R.)

Abstract: This article presents a thorough literature review of published designs of multiple-input multiple-output (MIMO) dielectric resonator antennas (DRAs) specifically designed for 5G applications. The performance of these designs is discussed in detail, considering various parameters such as gain, isolation, size, bandwidth, profile, and radiation characteristics. The primary objective of this work is to appreciate the significant progress made in this vital area of research. This article also aims to identify any existing gaps in the literature and provide potential directions for future work.

Keywords: MIMO; dielectric resonator antenna; 5G

Citation: Ahmad, H.; Jamaluddin, M.H.; Seman, F.C.; Rahman, M. MIMO Dielectric Resonator Antennas for 5G Applications: A Review. *Electronics* **2023**, *12*, 3469. https://doi.org/10.3390/electronics12163469

Academic Editors: Syed Muzahir Abbas and Yang Yang

Received: 16 July 2023
Revised: 5 August 2023
Accepted: 14 August 2023
Published: 16 August 2023

1. Introduction

Modern wireless communication heavily relies on 5G technology, which offers significant improvements compared to its predecessor, LTE/4G technology. 5G provides higher speeds, lower latency, increased reliability, and greater capacity. The bands used in 5G can be broadly categorized into two groups: sub-6 GHz and mm-wave (above 24 GHz). The sub-6 GHz band offers extensive coverage and is suitable for outdoor communication, while the mm-wave band has a narrower coverage and finds applications in indoor communication.

To meet the requirements of 5G, multiple-input multiple-output (MIMO) antennas are employed. In a MIMO antenna system, multiple antennas are compactly mounted on a common ground plane to reduce multipath fading, increase channel capacity, and improve link reliability. However, the design of MIMO antennas poses challenges such as reducing the size of antenna elements and managing the mutual coupling between them, which can degrade MIMO performance [1]. Previous studies have reported various printed antennas with different decoupling mechanisms for MIMO configurations, each with its own advantages and disadvantages.

In recent years, dielectric resonator antennas (DRAs) have gained popularity due to their appealing features [2]. Unlike printed antennas, DRAs do not suffer from conductor loss and surface waves at higher frequencies. These antennas are made from dielectric materials, resulting in high radiation efficiency. They offer simple design relations, a small size, a wide bandwidth, straightforward excitation methods, and easy fabrication [3,4]. Given the numerous advantages of DRAs, there has been increasing attention paid towards the design of MIMO DRAs for various applications [5].

This article focuses on MIMO dielectric resonator antennas designed for different 5G bands as reported in the literature. The published designs will be thoroughly analyzed, examining their advantages and disadvantages, acknowledging the contributions made, and identifying potential research gaps for future work in this rapidly evolving field.

2. Categorization of MIMO DRAs for 5G Applications

The classification of the MIMO DRAs for 5G applications can be performed by grouping them in different categories based on their operating 5G frequency band, type of DRAs, decoupling mechanism, polarization, and so on. In this work, we will review the literature by grouping the designs on the basis of isolation techniques as follows:

2.1. Diversity Techniques

The mutual coupling between the DRA elements in a MIMO antenna can be improved by utilizing the diversity techniques of spatial, polarization, and pattern diversity, which requires the careful placing of the DRAs with respect to each other. These techniques do not require any extra decoupling structure as opposed to the methods in which complex additional structures are incorporated in the designs.

2.1.1. Circularly Polarized Designs

MIMO CP DRAs are advantageous in terms of channel capacity, data rate, and link reliability. In this regard, a circularly polarized sub-6 GHz 5G MIMO antenna was proposed using two offset-fed rectangular DRAs in [6]. One DRA was excited by a conformal feed, while the other was excited by a microstrip-slot feed as shown in Figure 1. It has been demonstrated that an offset conformal feed produces two orthogonal degenerate modes, which satisfies one condition for circular polarization; however, it lacks a phase difference of 90° which is also a necessary condition for circular polarization. To cater to this, an offset notch was removed from the DRAs to attain phase-quadrature. The position of the feed and the notch have been optimized by a parametric analysis. The impedance bandwidth for the proposed design is between 5.15–6.12 GHz, while the Axial Ratio bandwidth is between 5.30–5.87 GHz. Pattern diversity ensured isolation by placing the DRAs on opposite sides of the substrate, radiating in different directions. This arrangement offered a compact size but with an increased profile.

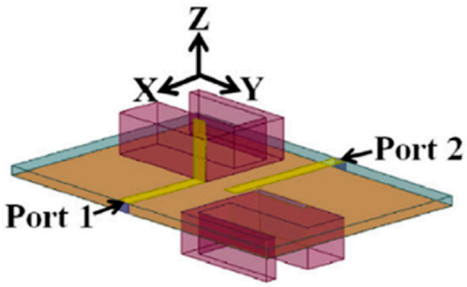

Figure 1. Offset-conformal-strip-fed MIMO DRA [6].

In [7], orthogonally placed graphene strips enabled circular polarization in a reconfigurable hemispherical MIMO DRA, but with added complexity. The feeding layer below the ground plane consists of a microstrip line that is surrounded by mushroom ridge-gap waveguide (RGW) unit cells. The RGW helps to stop the energy from the microstrip line from spreading and confines it right beneath the slot which eventually increases the gain to 10.3 dB. In [8], a two-element MIMO cylindrical DRA with circular polarization and spatial diversity for isolation improvement was presented with simulated results only.

In [9], circular polarization was achieved through modified annular ring slots and conformal feeding networks in a four-port cylindrical MIMO DRA. Polarization and pattern diversity were used for isolation. However, the design had an increased profile due to antennas on both sides of the substrate. In [10], circular polarization is achieved by a z-shaped slot in the ground plane which excites hybrid degenerate modes in the DRAs while the isolation between the DRAs is achieved through polarization diversity.

2.1.2. Multiband Designs

Multiband antennas are a useful tool for any professional who is on the road and connected to the critical communications community. These antennas can operate on multiple radio frequencies simultaneously while also providing coverage for other technologies. In this connection, a dual-band MIMO DRA with four ports for sub-6 GHz 5G applications was presented in [11]. It utilized rectangular DRAs excited by a slot in the patch radiator placed beneath the DRA on a substrate backed by the ground plane, as shown in Figure 2. The design achieved resonances at 3.3 GHz and 3.9 GHz, with impedance bandwidths ranging from 2.86–3.48 GHz and 3.67–4.25 GHz. Mutual coupling was reduced by orthogonal placement of adjacent DRAs. Triangular slots in the feed enabled dual-band operation in the rectangular MIMO DRA presented in [12]. The orthogonal placement of adjacent DRAs improved isolation, utilizing polarization diversity. However, the design has the drawback of limited impedance bandwidth.

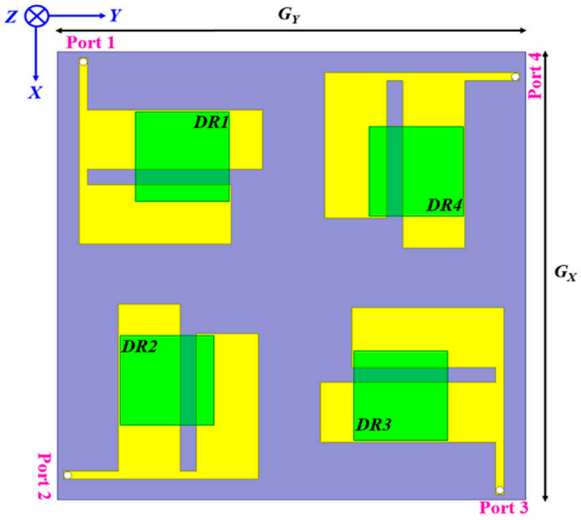

Figure 2. MIMO DRA with patch radiator [11].

A hybrid MIMO DRA with multiband characteristics was introduced in [13]. It used two rectangular DRAs on a substrate with a partial ground plane. The design achieved dual-band operation (3.4–4.32 GHz and 4.96–5.05 GHz) through a microstrip feeding network and parasitic patch. The partial ground plane widened the bandwidth and improved matching. The orthogonal placement of DRAs and the feeding network resulted in isolation exceeding 22 dB for both bands.

In [14], a compact MIMO DRA for 5G mm-wave applications was proposed. It utilized two rectangular DRAs on opposite sides of a substrate, fed by coplanar waveguide feeds with ground plane slots. Operating at 28 GHz and 38 GHz, the antenna achieved gains of 6.2 dBi and 7.57 dBi, respectively. The impedance bandwidth was approximately 5 GHz (18% and 13% at 28 GHz and 38 GHz). The design improved isolation by 27 dB without additional structures for mutual coupling reduction and with a reduced structural complexity, although the height was increased due to the proposed arrangement.

In [15], a dual-band MIMO DRA for vehicular applications was presented. It used rectangular microstrip lines with S-shaped apertures to excite higher order modes. Ring-shaped dielectric resonators provided wider bandwidth, and the asymmetric aperture generated multiple resonances and circular polarization. The design achieved LHCP and RHCP polarization diversity with high gain (8.1 dBi) and radiation efficiency (>90%) by using mirrored apertures and a conducting plate for isolation. A simulated cylindrical MIMO DRA utilizing spatial diversity for isolation was presented in [16], which employs microstrip feed with a circular patch for dual-band operation.

In [17], a dual-band MIMO dielectric resonator antenna (DRA) for 5G mm-wave applications was presented. Four rectangular DRAs were arranged in a cross-shaped

structure in which each DRA was excited by a substrate integrated waveguide through a slot as shown in Figure 3. The impedance bandwidth obtained was between 24.5–27.5 GHz and 33–37 GHz. Polarization diversity isolated adjacent DRAs, while spatial diversity reduced coupling between DRAs in parallel. The design achieved an isolation greater than 22 dB and 17 dB (for the lower and upper bands, respectively) and high gain (9.9 dBi) with high efficiency (>96%) across the operating bandwidth.

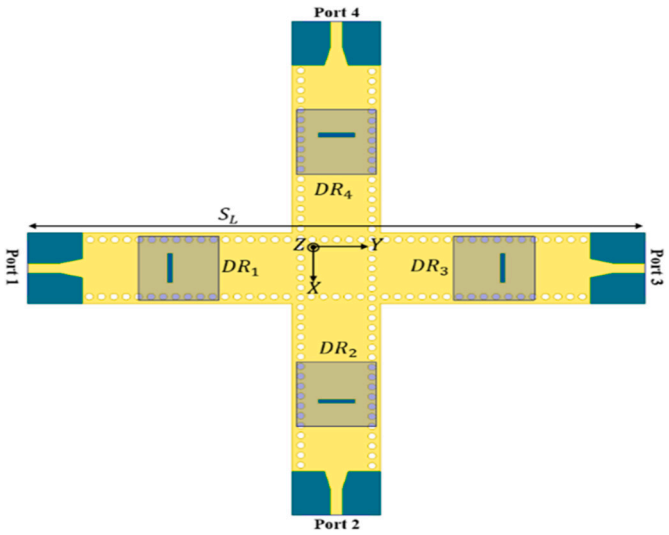

Figure 3. SIW-fed MIMO DRA [17].

In [18], a dual-band MIMO DRA for the sub-6 GHz 5G and other bands was presented. It utilized five rectangular DRAs arranged cubically with PEC layers, achieving resonances at 3.5 GHz and 5.9 GHz. An offset coaxial probe feed was used, and orthogonal placement reduced coupling for isolation exceeding 25 dB. The design offered greater capacity and a smaller footprint but occupied a large volume.

In [19], a two-port dual-band antenna was presented, consisting of a slot antenna and a DRA on separate substrates. The slot antenna operated at 5.2 GHz (5.15–5.25 GHz bandwidth), while the DRA operated at 24 GHz (23.87–24.36 GHz bandwidth). Maximum gains achieved were 3.93 dBi (lower band) and 6.32 dBi (higher band). Port isolation exceeded 35 dB through orthogonal feeding using polarization diversity. However, the design had limitations such as a narrow bandwidth and fabrication complexity.

2.1.3. High Gain Designs

High gain designs are advantageous in term of their high level of functionality and security. These antennas have a narrow radio beam, which increases the strength of the signal. A MIMO DRA for 5G mm-wave applications utilizing eight cylindrical DRAs on a substrate, excited by rectangular slots, was presented in [20]. Four DRAs formed two linear arrays in the proposed structure. Isolation between DRAs was achieved by tilting array beams in opposite directions for pattern diversity. A peak gain greater than 7 dBi is achieved by the proposed array with a radiation efficiency of 80%. Advantages include high gain, good isolation, and a compact size without additional structures for mutual coupling reduction, with the drawback of increased sidelobe levels. A high gain of 9.43 dBi was achieved by a 3 × 3 MIMO array in [21].

In [22], a compact MIMO DRA with pattern diversity has been presented. The proposed design consists of two epsilon-shaped DRAs placed on top of a substrate facing each other and two cylindrical DRAs between the epsilon-shaped DRAs. The distance between the epsilon shaped DRAs is less than a wavelength and so is the distance between the cylindrical DRAs. As a result, the entire structure acts as a single DRA. It achieved

high gain (6.5 dBi), efficiency (97%), and a compact size with enhanced isolation using rectangular slots.

In [23], a wideband MIMO DRA for sub-6 GHz 5G applications was proposed. It featured A-shaped DRAs on a substrate, with conformal feeds. Orthogonal placement reduced mutual coupling, achieving an isolation greater than 20 dB. The wide impedance bandwidth achieved by perturbing the triangular DRA into the proposed A-shape ranges between 3.2–6 GHz with a measured gain ranging between 6.03–7.45 dBi. In [24], a simulated design was presented, utilizing spatial diversity for decoupling, and improved gain by exciting DRA in a higher-order mode.

A simulated four-port, closely spaced MIMO DRA consisting of four arrays of sixteen cylindrical DRAs utilizing pattern diversity for 5G mm-wave applications was presented in [25]. With the proposed array, a gain of 10 dBi was achieved. A similar design with two ports consisting of two arrays each with four DRAs, achieving a gain of 9 dBi, was proposed in [26]. In [27], polarization diversity is utilized to reduce the mutual coupling in a four-port wideband MIMO antenna for 5G mm-wave applications where the impedance bandwidth ranges between 26.5 GHz to 43.7 GHz and the maximum gain is greater than 8 dBi.

2.1.4. High Capacity Designs

A sixteen-port eight-element MIMO DRA with a built-in decoupling mechanism was introduced in [28]. The design comprised four DRAs on the top side and four DRAs beneath, all placed on an FR4 substrate as shown in Figure 4. Each top DRA was excited by two orthogonally positioned CPW-fed conformal strip lines, while each bottom DRA was excited by two orthogonally positioned microstrip-fed conformal strip lines. This arrangement formed an eight-element MIMO, enabling a sixteen-port MIMO configuration to enhance the channel capacity. Isolation between the DRAs was achieved through all the three diversity techniques, i.e., polarization, pattern, and spatial diversity. The increased profile due to the placement of DRAs on both sides of the substrate is a major disadvantage.

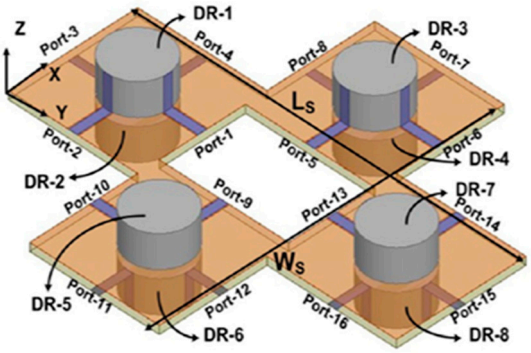

Figure 4. Sixteen-port eight-element MIMO DRA [28].

In [29], an eight-port MIMO antenna with a quad-directional pattern was presented. The design featured four cylindrical DRAs placed in a box configuration radiating in four directions, with each DRA being excited by probe feeding and conformal-strip feeding, achieving orthogonal feeding and improving isolation. In [30], an eight-port MIMO antenna exhibiting high channel capacity utilizes spatial diversity and polarization diversity to achieve an isolation greater than 12 dB within an operating frequency of 3.4–3.6 GHz. The design has the advantage of mutual coupling reduction without incorporating any structure but with an increased size.

2.1.5. High Isolation Designs

In [31], a quad-port MIMO DRA has been presented for 5G mm-wave applications. The proposed design consists of a rectangular DRA that is mounted on a substrate integrated waveguide and excited differentially through two narrow slots on the top surface of SIW.

The DRA resonates at 28 GHz with an impedance bandwidth of 27.5–28.4 GHz. The radiators in the MIMO configuration are arranged in such a manner that the DRAs that are adjacent to each other are isolated from each other due to orthogonal polarization, while the DRAs that are placed opposite to each other are isolated from each other due to the larger gap between them. Thus, the proposed design utilizes a combination of polarization and spatial diversity to attain a high isolation greater than 40 dB in the entire band of operation.

In [32], a four-port MIMO antenna achieves an isolation greater than 25 dB by employing polarization and spatial diversity to operate at the 35 GHz mm-wave band. A similar approach has been used in [33] for obtaining an isolation greater than 27 dB in an SIW-fed MIMO DRA operating in the mm-wave band of 26.64–28.55 GHz. A comparison of several designs reported so far utilizing diversity techniques for mutual coupling reduction has been given in Table 1.

Table 1. Comparison of reported designs utilizing diversity techniques.

Ref.	Gain (dBi)	Bandwidth (%)	Isolation (dB)	Polarization
[6]	4.7	17.2	17.1–27.6	Circular
[11]	5.8, 6.2	19.5, 14.6	>20, >26	Linear
[17]	9.1, 9.9	11.5, 12	>22, >17	Linear
[23]	6.03–7.45	60.8	>20	Linear
[25]	10	6.7	>15	Linear
[28]	5–6.5	8.8	>17	Linear
[31]	4.2	3.2	>40	Linear
[7]	5	30.2	>22	Circular

From the reported designs utilizing diversity techniques for mutual coupling reduction, it can be observed that high isolation can be achieved only if a combination of diversity techniques is employed. Moreover, diversity techniques will not improve the gain or bandwidth, or achieve circular polarization. Separate strategies need to be applied to the DRAs in a MIMO configuration in order to achieve the desired characteristics.

2.2. Periodic Structures

The mutual coupling between DRAs in a MIMO configuration can be significantly reduced by incorporating periodic structures such as metamaterials, EBGs, FSS, and metasurfaces. As opposed to the diversity techniques, these structures considerably enhance the isolation by limiting the coupling energy between the DRAs, though the design complexity is increased.

2.2.1. Circularly Polarized Designs

In [34], a two-element cylindrical MIMO dielectric resonator antenna for the sub-6 GHz band was presented. Mutual coupling was reduced using a carefully designed metasurface on top of the DRAs, which also generated circular polarization. The design operated at 3.81 GHz (3.86–4.23 GHz bandwidth), achieving over 20 dB isolation, 4 dBi gain, and over 90% radiation efficiency. The compact design allowed the close placement of DRAs, but with an increased profile and complexity in fabrication with a low gain.

In [35], a circularly polarized, wideband MIMO DRA was presented, featuring two rectangular DRAs on an FR4 substrate fed by microstrip lines. Wideband CP response was achieved by truncating the opposite edges of the DRAs. A cross-ring-shaped slot on the ground plane generated CP fields. Mutual coupling between the two DRAs was reduced using an electromagnetic band-gap surface etched on the ground plane as shown in Figure 5. Isolation exceeded 26 dB across the operating bandwidth. The design offered a wideband CP, simple feeding structure, and good isolation but a low gain.

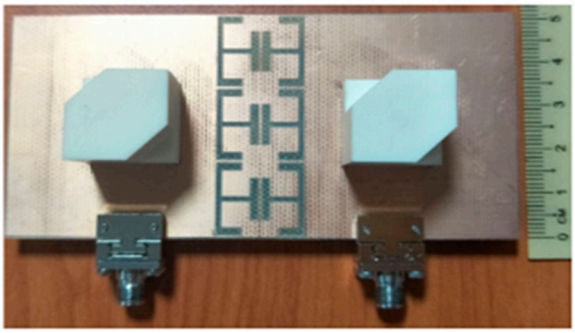

Figure 5. CP MIMO DRA with EBG on ground plane [35].

2.2.2. High Gain Designs

In [36], a triple-band MIMO DRA for sub-6 GHz 5G applications was presented. It featured six cylindrical DRAs on an FR-4 substrate, grouped with different heights but the same diameters to generate three resonant frequencies. CPW-fed conformal strips excited the DRAs, while a partially reflecting surface (PRS) reduced mutual coupling. The PRS increased the peak gain by 2 dB but decreased radiation efficiency (90% to 80%). Limitations included lower radiation efficiency, reduced impedance bandwidth, increased side lobe levels at higher frequencies, and an increased profile due to the minimum distance required for the PRS above the DRAs. Another design utilizing metamaterial for gain enhancement on top of the MIMO DRA for 5G mm-wave applications was proposed in [37]. The metamaterial served to reduce the mutual coupling between adjacent DRAs and assisted in achieving a gain greater than 7 dBi for the proposed design.

In [38], a MIMO DRA with an FSS wall for the 60 GHz mm-wave band was presented as shown in Figure 6. It included two cylindrical DRAs on a substrate, excited through ground plane slots fed by microstrip lines. The FSS wall reduced mutual coupling using Jerusalem-cross- and fan-shaped structures, achieving over 30 dB isolation, 1.5 dB increased gain, and over 90% radiation efficiency. A drawback was the tilted radiation pattern from the boresight direction.

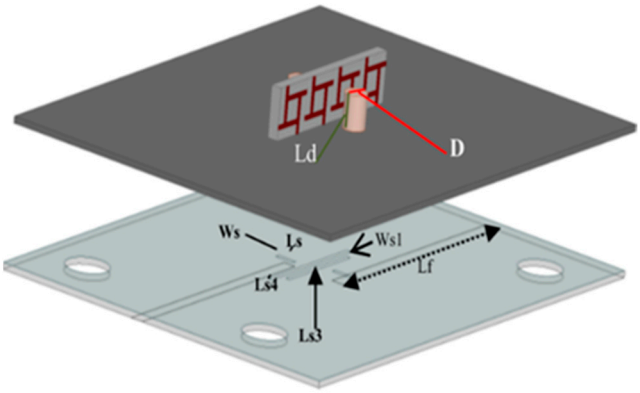

Figure 6. MIMO DRA with FSS wall [38].

In [39], a 60 GHz MIMO DRA with a metasurface was presented. It featured two cylindrical DRAs on an upper substrate, excited through rectangular slots and fed by microstrip feedlines on a lower substrate. A metasurface unit cell consisting of split ring resonators with gaps reduced mutual coupling. The design achieved high isolation (>18 dB), improved gain (7.9 dBi), and efficiency (91%) at 60 GHz, but with a tilted main beam in the H-plane.

2.2.3. High Isolation Designs

In [40], a hybrid isolator was presented for reducing mutual coupling in a two-element cylindrical MIMO DRA. The hybrid isolator, consisting of an EBG structure and a choke absorber, was placed between the DRAs as shown in Figure 7. Operating at 60 GHz (59.3–64.8 GHz bandwidth), the design achieved high isolation (>29 dB, up to 49 dB) in the entire operating band. The limitations of the proposed design are low radiation efficiency, an increased profile due to the choker absorber, and the shift of the direction of the main beam in the H-plane.

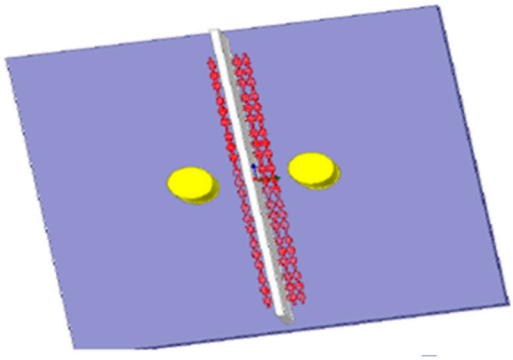

Figure 7. Hybrid-isolator-based MIMO [40].

In [41], a mutual reduction technique for a 60 GHz mm-wave MIMO DRA was proposed. It featured two cylindrical DRAs on a substrate, excited through a rectangular slot in the ground plane. A metamaterial polarization rotator (MPR) wall between the DRAs achieved high isolation by reducing mutual coupling on an average of 16 dB without affecting the radiation pattern. Limitations included an increased profile due to the multilayered structure, design complexity, and lower radiation efficiency (92% to 88%) when the MPR wall was employed.

In [42], a compact EBG structure was proposed to reduce mutual coupling between DRAs in a 60 GHz MIMO antenna. It featured two cylindrical DRAs on a substrate, excited through ground plane slots by microstrip feedlines. Six unit cells of the proposed EBG structure placed between the DRAs achieved an average isolation reduction of 13 dB, with the minimum and maximum isolation exceeding 15 dB and 30 dB, respectively. The design had the drawbacks of low gain and a 30° tilted radiation pattern in the E-plane. A comparison of several studies utilizing different periodic structures for mutual reduction has been given in Table 2.

Table 2. Comparison of reported designs utilizing periodic structures.

Ref.	Gain (dBi)	Bandwidth (%)	Isolation (dB)	Polarization	Decoupling Structure
[35]	4.83	25.9	>26	Circular	EBG
[39]	7.9	11.6	>18	Linear	Metasurface
[40]	8.1	8.8	29–49	Linear	EBG and choke absorber
[37]	>7.5	7.9	Up to 29.34	Linear	Metamaterial

The reported designs utilizing periodic structures for mutual coupling reduction indicate that high isolation can be achieved with such structures. Other desired performance characteristics including a high gain, the desired bandwidth, and circular polarization can also be achieved by carefully designing the periodic structures. However, a major drawback of such structures is the design complexity.

2.3. Other Decoupling Structures

The mutual coupling between the DRAs in a MIMO antenna can also be reduced by other decoupling structures which offer simpler designs as compared to periodic structures. Various such decoupling structures have been reported in the literature which will be discussed in this section.

2.3.1. Compact Designs

In [43], a MIMO DRA with port and radiation pattern decoupling was presented. The design utilized the principle of inducing a current in two adjacent DRAs through metallic posts. When a single DRA was excited, the induced current canceled out the fields in the adjacent DRA, achieving decoupling. Using the above concept, two designs were proposed, one with H-plane decoupling and the other with E-plane decoupling, as shown in Figure 8. The advantage of the proposed design is that it is very compact, as the two DRAs are placed without any spacing between them. A drawback, however, is the low bandwidth. In [44], a simulated substrate integrated MIMO DRA antenna for mm-wave applications was proposed in which the isolation between the DRAs was achieved using metallic vias and rectangular strips.

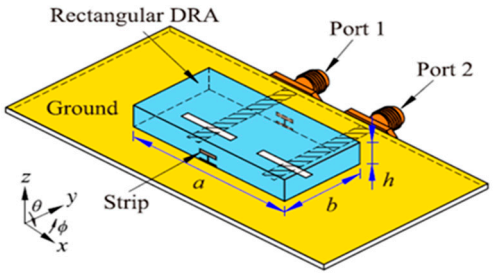

Figure 8. H-plane-decoupled MIMO DRA [43].

In [45], a decoupling method was proposed for a single-element MIMO DRA at 28 GHz. Techniques involving embedded metallic sheets (for E-plane coupling) and sidewall attachments (for H-plane coupling) reduced mutual coupling by suppressing EM wave concentration. The proposed design is very compact since a single-element DRA is utilized but with the drawback of limited bandwidth. In the simulated design of [46], decoupling was achieved in a closely spaced half-volume MIMO DRA by incorporating an inductor between the feeding microstrip lines.

In [47], conductive metallic strips were employed on the adjacent walls of the rectangular MIMO DRA to reduce mutual coupling in the H-plane as shown in Figure 9. The metallic strips suppressed the fields of the adjacent excited DRA from reaching the feed of the undriven DRA. The proposed design has a simple and compact design but with a smaller bandwidth. Similarly, Ref. [48] presented a decoupling method using metallic strips on adjacent and opposite walls for a mm-wave rectangular MIMO DRA to achieve an isolation greater than 50 dB.

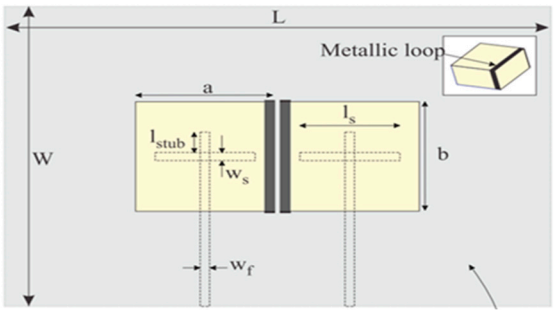

Figure 9. MIMO DRA with metallic strips on adjacent walls [47].

A starfish-shaped single-element compact MIMO was proposed in [49] with a degenerated ground structure for improved isolation and bandwidth. Another single-element cylindrical four-port MIMO DRA for mm-wave 5G applications employed a degenerated ground structure for isolation enhancement in [50]. Similarly, isolation was improved by utilizing slots in the ground plane in [51].

In [52], a technique to reduce mutual coupling in MIMO DRAs for 5G mm-wave applications was proposed. The design featured two rectangular DRAs on a Rogers substrate, excited by microstrip-fed slots as shown in Figure 10. Printed metallic strips on the DRAs' upper surface shifted the coupling field to the side, achieving over 24 dB isolation across the bandwidth without affecting the radiation pattern. The compact design required no additional space between the DRAs. However, the utilization of metallic strips decreased the gain and impedance bandwidth of the DRAs compared to the absence of the strips.

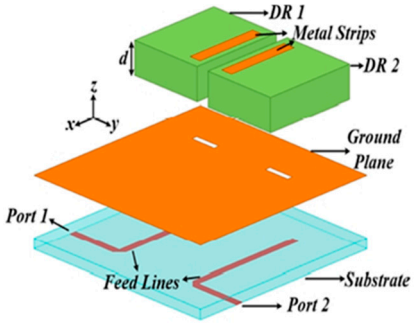

Figure 10. MIMO DRA with metal strips [52].

2.3.2. Circularly Polarized Designs

In [53], an A-shaped conformal metal strip achieved circular polarization while an S-shaped slot reduced mutual coupling in a sub-6 GHz rectangular MIMO DRA. The design operated at a resonant frequency of 3.72 GHz with an impedance bandwidth of 3.57–4.48 GHz. In [54], a two-element cylindrical MIMO DRA has been presented for 5G and X-band applications. The proposed design consists of a mirror S-shaped radiator that produces linearly polarized waves at 4.4–5.05 GHz and 7.85–8.43 GHz, while a cylindrical DRA placed in the center of the S-shaped radiator works to generate CP in 9.05–10.10 GHz band. For mutual coupling reduction between the two antennas, a partial ground plane with a slot has been used. The bottom side also consists of an elliptical radiator with a T-shaped slot to achieve an isolation greater than 20 dB in the operating bandwidth.

In [55], a dual-band circularly polarized MIMO DRA for sub-6 GHz 5G applications was presented. The design featured two ring DRAs on a substrate, excited by arc-shaped microstrip feed lines with conformal probes as shown in Figure 11. The probes generated orthogonal hybrid modes, enabling circular polarization. Improved isolation between ports was achieved by a rectangular slot in the ground plane. In [56], a MIMO DRA with CP agility for 5G applications was introduced. The design featured two DRAs on a hexagonal substrate, fed by L-shaped microstrip lines and conformal probes. The substrate reduced the antenna size, while the L-shaped feed lines and conformal probes enabled circular polarization.

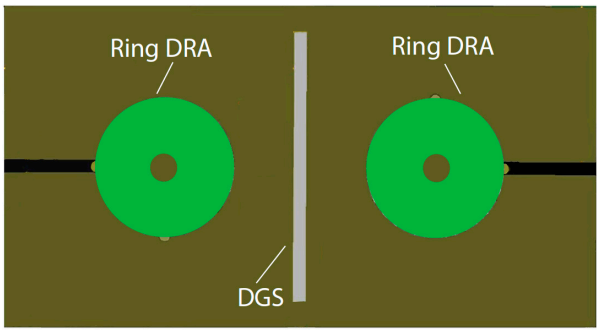

Figure 11. Geometry of dual-band CP MIMO DRA [55].

2.3.3. Broadband Designs

In [57], a four-element MIMO DRA was presented utilizing a linear array of 1 × 4 rectangular DRAs on small separated ground planes placed above a larger common ground plane. By adjusting the dimensions and distance of the small ground planes, mutual coupling between the DRAs was reduced. The design achieved a gain of 8.2 dBi and offered high isolation, an improved front-to-back ratio, and a wider bandwidth (3.37–4.10 GHz) compared to conventional DRAs. However, it has an increased profile and complexity.

In [58], a dual-element wideband triangular DRA for MIMO applications has been presented. The proposed design consists of two triangular DRAs that are fed by coaxial probes. Triangular DRAs have less size as compared to rectangular and cylindrical DRAs with the same permittivity and height operating at the same resonant frequency. The mutual coupling between the DRAs have been reduced by placing four metal vias between the DRAs. The position of the vias have been optimized to achieve maximum isolation and, at the same time, provide a wide bandwidth of 4.67–9.50 GHz (67.5%).

2.3.4. Multiband Designs

In [59], an on-chip MIMO DRA with multiband characteristics has been presented for mm-wave applications. The proposed design consists of two rectangular DRAs made from a silicon wafer and placed in a substrate of the same material. The energy to the DRAs was coupled by using coplanar waveguides. The mutual coupling between the DRAs was reduced by approximately 5–22 dB when a dielectric wall was placed between the DRAs. The resonant frequencies of the proposed design are 26, 36, 41, 47, and 52 GHz, with impedance bandwidths of 16%, 6.6%, 3.8%, 8.9%, and 5.5%, respectively.

In [60], a hybrid MIMO DRA operating in four bands was presented. The design comprised two cylindrical DRAs fed by a tapered rhombic ring-shaped feed, achieving quad-band operation. The resonant frequencies for the proposed design were 2.5 GHz, 5.09 GHz, 6.8 GHz, and 9 GHz, and the impedance bandwidth for these bands were 14.6%, 10.7%, 4.2%, and 5.3%, respectively. Mutual coupling between the radiators was reduced using a partial ground plane with a center slot and two L-shaped slots. The drawbacks were low bandwidth in all four bands, and decreased gain and efficiency due to degenerated ground. In [61], a quad-band MIMO antenna with a perforated DRA for achieving four bands and ground plane slots for enhancing isolation was simulated. The proposed design resonates at 2.95 GHz, 3.93 GHz, 4.8 GHz, and 5.8 GHz, with impedance bandwidths of 2.83–3.07 GHz, 3.79–4.04 GHz, 4.7–4.9 GHz, and 5.72–5.86 GHz, respectively.

The design and numerical analysis of a rectangular terahertz (THz) dielectric resonator (DR) antenna are presented in [62] recently. The study is presented with the DR aspect ratio chosen in a way that allows the antenna to operate in four modes with a triple-band response. The graphene strips have also been added to the DRs' top radiating surface. By carefully choosing the chemical potential of graphene, it is possible to manipulate the resonant modes of an antenna to produce either a large single-band or triple-band response. The antenna continues to provide the triple-band response operating at frequencies of 2.10–2.33, 2.56–2.65, and 2.77 THz.

2.3.5. High Isolation Designs

In [63], a decoupling mechanism was proposed to improve the isolation of DRAs in a MIMO arrangement as shown in Figure 12. A dielectric superstrate placed above the DRAs effectively weakened the interaction between adjacent DRAs, reducing mutual coupling. The proposed structure increased isolation by 25 dB, improved gain and efficiency, and maintained polarization purity without modifying the DRAs' resonant frequency. However, the design increased the MIMO profile and reduced the impedance bandwidth.

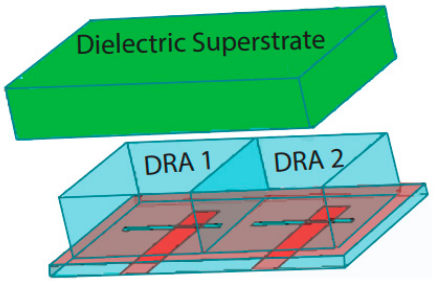

Figure 12. MIMO DRA with dielectric superstrate [63].

In [64], metallic vias were used to reduce mutual coupling in both H-plane- and E-plane-coupled MIMO DRAs for 5G mm-wave applications. The design achieved over 30 dB isolation, compactness, and improved gain, but required the optimization of the resonant frequency due to the vias' effect. A 60 GHz MIMO DRA with a dielectric superstrate for gain enhancement was presented in [65]. The mutual coupling between the DRAs was reduced by etching a slot from the ground plane and placing a metallic strip between the DRAs, achieving an isolation greater than 20 dB for the entire band of interest. A similar level of isolation was achieved by a four-port rectangular MIMO DRA utilizing vertical metal plates for minimizing mutual coupling in [66]. A comparison has been made for several decoupling structures with their performance parameters as shown in Table 3.

Table 3. Comparison of reported designs utilizing different decoupling structures.

Ref.	Gain (dBi)	Bandwidth (%)	Isolation (dB)	Polarization	Decoupling Structure
[47]	3.5	7.5	Up to 28	Linear	Metallic strips
[49]	2.97	79	>20	Linear	Defected ground structure
[53]	6	36.63	Up to 28.25	Circular	Defected ground structure
[57]	8.2	19.5	>25	Linear	Decoupling ground
[60]	2.18, 4.59, 4.11, 4.75	14, 10, 4, 5	Up to 22, 34, 30, 18	Linear	Defected ground structure
[63]	5.6	6.6	>25	Linear	Dielectric superstrate
[45]	6.4	3.4	Up to 23.45	Linear	Metallic sheets
[66]	4.09	10.4	>20	Linear	Vertical metal plates

From the designs reported in this section, it can be observed that a careful choice needs to be made when employing a particular decoupling structure for isolation enhancement, as some structures can have a pronounced effect on different performance parameters such as gain, bandwidth, and polarization.

2.4. Self-Decoupling Techniques

The techniques discussed so far enhance isolation through decoupling structures or the strategic placement of DRAs, but suffer from increased design complexity and size. This section explores mutual coupling reduction techniques that provide isolation without additional structures and with a built-in isolation mechanism. Most reported designs in this category are compact single-element DRAs, offering reduced complexity and size.

2.4.1. Single-Element Designs

In [67], a compact Y-shaped MIMO DRA was proposed for sub-6 GHz 5G applications. It consisted of three rectangular DRAs merged at a 120° angle, forming a Y-shape on a circular substrate with a ground plane as shown in Figure 13. Each arm was fed by a conformal strip, resulting in three ports. The mutual coupling was reduced by directing each port's main beam in a different direction. However, limitations included low radiation efficiency and isolation. In [68], the rectangular DRA was transformed into a plus-shaped design to improve isolation by removing portions of the DRA with strongly interfering fields.

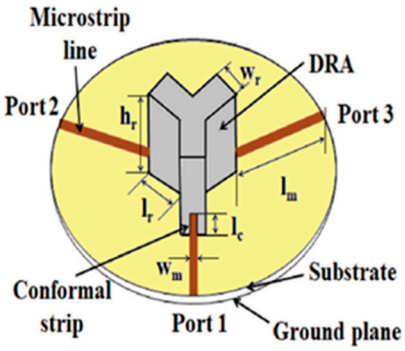

Figure 13. 3-D view of Y-shaped MIMO DRA [67].

In [69], a triple-band dual-polarized MIMO dielectric resonator antenna (DRA) was introduced for 5G and other wireless applications. The design featured a square DRA on an FR4 substrate, excited through rectangular slots by two orthogonal L-shaped monopole microstrip feeds as shown in Figure 14. Resonances were achieved at 1.7 GHz, 2.6 GHz, and 3.6 GHz, with respective impedance bandwidths of 1.63–1.84 GHz (12%), 2.43–2.71 GHz (10.89%), and 3.27–3.75 GHz (13.68%), respectively. The maximum isolation reached 20 dB for all the three bands. The design offered simplicity, dual-band operation, and ease of fabrication.

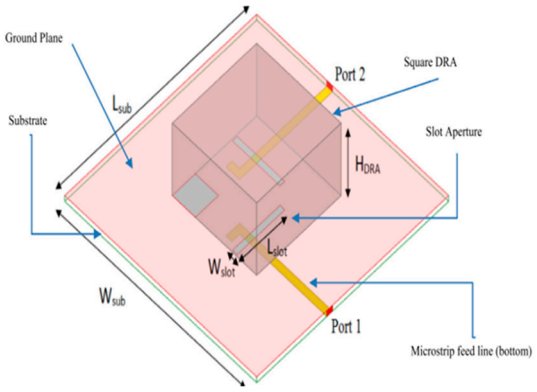

Figure 14. 3-D view of the proposed MIMO [69].

In [70], isolation between the ports of a single-element triangular MIMO DRA was improved by removing a semi-cylindrical portion of the DRA between the ports. A simulated two-port MIMO dielectric resonator antenna for 5G mm-wave applications presented in [71] consisted of two p-shaped dielectric resonators that were excited by a microstrip line through a slot, improving isolation and offering a compact size.

2.4.2. Multiple-Element Designs

In [72], isolation between the DRAs was achieved by exciting higher-order modes with the same radiation pattern as the active DRA. The proposed design had a resonant frequency of 5.25 GHz and an impedance bandwidth of 4.89–5.42 GHz, with a gain ranging

from 7 to 7.8 dBi and radiation efficiency of 85–95%. The method offered a compact, low-loss, low-complexity, and cost-effective design, although the size of the antenna increased due to the utilization of higher-order modes.

The investigation of a unique self-decoupling technique for MIMO dielectric resonator antenna (DRA) arrays are presented in [73]. This approach is founded on the conformal strip's transmission properties that support the DRA. When the strip-fed DRA operates, it is discovered that a higher-order mode, TE_{113} mode, operates. This self-decoupling technique can be used with 2-D MIMO planar arrays, in addition to 1-D H- and E-plane coupled MIMO linear arrays. A 2 × 2 MIMO planar DRA array prototype is simulated, processed, and tested to confirm its viability. Figure 15 shows the design of the DRA structure and Figure 16 shows the corresponding S-parameter response. A comparison of several reported designs of self-decoupled MIMO DRAs for 5G applications has been provided in Table 4.

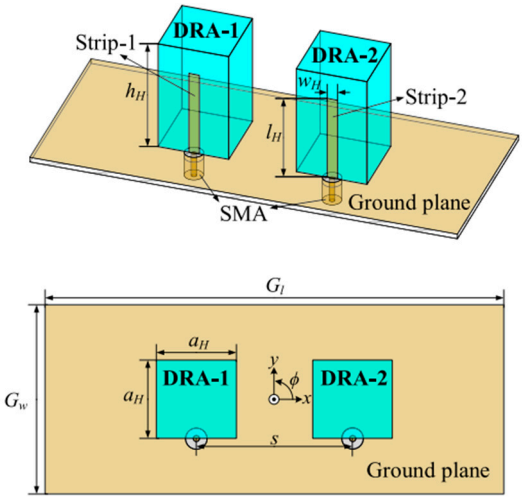

Figure 15. Configuration of the investigated coupled 1 × 2 MIMO DRA array [73].

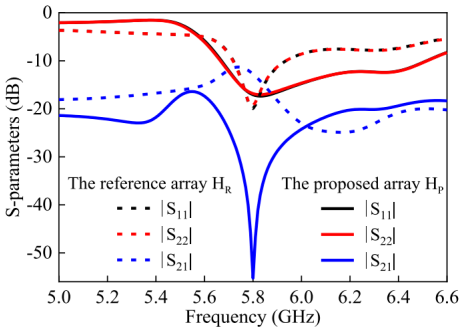

Figure 16. Simulated S-parameter response from the structure in [73].

Table 4. Comparison of self-decoupled designs.

Ref.	Gain (dBi)	Bandwidth (%)	Isolation (dB)	Polarization
[67]	8	64	>10	Linear
[68]	5.12	11.6	Up to 15	Linear
[69]	5.5, 5.9, 6.9	12, 10.89, 13.68	Up to 20	Linear
[72]	7–7.8	10.2	Up to 60	Linear

The self-decoupled designs have the advantage that no extra decoupling element is required for isolation, which reduces the design complexity and offers a compact design. A proper choice of the technique can provide high isolation, bandwidth, or gain, as per the

designer's requirement. The authors, however, could not find any design that achieved circular polarization with a self-decoupling technique.

3. Discussion and Future Work Suggestions

The decoupling techniques reported for reducing mutual coupling in MIMO DRA for 5G have been compared in Table 5 below. Each technique has its own advantages and shortcomings, and, therefore, a careful decision needs to be made when choosing a decoupling technique for achieving the desired results.

Table 5. Comparison of various decoupling techniques.

Decoupling Technique	Advantages	Shortcomings
Diversity techniques	Easy to implement Less design complexity	Moderate isolation Increases the size and profile of MIMO
Electromagnetic band-gap structures	High isolation Can increase gain	Design complexity Shifts main beam Increases size of MIMO
Metamaterials	High isolation	Increases size of MIMO Design complexity
Metasurfaces	High isolation Can increase gain	Increases size of MIMO Shifts main beam from boresight direction Design complexity
Frequency selective surfaces	High isolation Can increase gain	Increases size of MIMO Design complexity Beam tilting from boresight direction
Conformal metal strips	Good isolation Compact design Ease of fabrication	Low bandwidth Low gain and efficiency Shifts the original resonance frequencies of DRAs
Dielectric superstrate	High isolation Can increase gain and efficiency Restores the tilt in main beam	Fabrication complexity Increases profile of MIMO
Metallic vias	Good isolation Does not occupy extra space	Lowers gain and efficiency Shifts resonance frequency Difficult to drill holes inside DRAs
Defected ground structures	Good isolation May improve bandwidth Does not increase profile	Lowers gain and efficiency due to backward radiation

The literature review has identified several research gaps that can be explored in future work:

- Limited circular polarization: Only a few MIMO dielectric resonator antenna (DRA) designs for 5G exhibit circular polarization, particularly in the mm-wave band.
- Increased edge–edge separation: When an isolating structure is inserted between the DRAs, the distance between their edges becomes large, impacting the overall compactness of the design.
- Lack of structural novelty: The majority of reported designs do not introduce novel structures for the DRAs, suggesting a need for more innovative approaches.
- Compactness challenges: It is challenging to achieve a compact structure when an isolating structure, which occupies more space, is placed between the DRAs.
- Limited bandwidth: Most designs have reported a small bandwidth, indicating the need for improvements to achieve wider frequency coverage.

- Profile reduction: Many designs have not made efforts to reduce the profile of MIMO antennas, highlighting a potential area for improvement.

The utilization of DRAs for 5G MIMO applications is still a developing area of research as evident from the number of publications in this area as compared to the proposed designs utilizing other antenna types for 5G MIMO arrangements. Addressing the above-mentioned research gaps can contribute to advancements in MIMO DRA designs for 5G applications.

4. Conclusions

An extensive literature review on multiple-input multiple-output (MIMO) dielectric resonator antennas (DRAs) designed for 5G applications was presented. The performance of the reported designs in terms of gain, isolation, size, bandwidth, profile, and radiation characteristics was discussed. The article also aimed to highlight the advancements in this research area, identify gaps in the existing literature, and suggest potential directions for future research.

Author Contributions: H.A., M.H.J. and F.C.S. were involved in the ideation of the study; H.A., M.H.J. and M.R. performed the literature search and data analysis; H.A., M.H.J., F.C.S. and M.R. drafted and revised the work. All authors have read and agreed to the published version of the manuscript.

Funding: This research received no external funding.

Data Availability Statement: Not applicable.

Conflicts of Interest: The authors declare no conflict of interest.

References

1. Sharawi, M.S. Printed multi-band MIMO antenna systems and their performance metrics [wireless corner]. *IEEE Antennas Propag. Mag.* **2013**, *55*, 218–232. [CrossRef]
2. Petosa, A.; Ittipiboon, A. Dielectric resonator antennas: A historical review and the current state of the art. *IEEE Antennas Propag. Mag.* **2010**, *52*, 91–116. [CrossRef]
3. Keyrouz, S.; Caratelli, D. Dielectric Resonator Antennas: Basic Concepts, Design Guidelines, and Recent Developments at Millimeter-Wave Frequencies. *Int. J. Antennas Propag.* **2016**, *2016*, 6075680. [CrossRef]
4. Mongia, R.K.; Bhartia, P. Dielectric resonator antennas—A review and general design relations for resonant frequency and bandwidth. *Int. J. Microw. Millim.-Wave Comput.-Aided Eng.* **1994**, *4*, 230–247. [CrossRef]
5. Singhwal, S.S.; Matekovits, L.; Kanaujia, B.K.; Kishor, J.; Fakhte, S.; Kumar, A. Dielectric Resonator Antennas: Applications and developments in multiple-input, multiple-output technology. *IEEE Antennas Propag. Mag.* **2022**, *64*, 26–39. [CrossRef]
6. Sahu, N.K.; Das, G.; Gangwar, R.K. Circularly polarized offset-fed DRA elements & their application in compact MIMO antenna. *Eng. Sci. Technol. Int. J.* **2022**, *28*, 101015.
7. Malhat, H.A.; Zainud-Deen, S.H.; El-Hemaily, H.; Hamed, H.A.; Ibrahim, A.A. Reconfigurable Circularly Polarized Hemispherical DRA Using Plasmonic Graphene Strips for MIMO Communications. *Plasmonics* **2022**, *17*, 765–774. [CrossRef]
8. Kumari, P.; Kumari, T.; Suman, K.K.; Gangwar, R.K.; Chaudhary, R.K. A Circularly Polarized Sub-6 GHz MIMO Antenna for 5G Applications. In Proceedings of the 2022 IEEE International Symposium on Antennas and Propagation and USNC-URSI Radio Science Meeting (AP-S/URSI), Denver, CO, USA, 10–15 July 2022.
9. Sahu, N.K.; Das, G.; Gangwar, R.K.; Rambabu, K. An arrangement for four-element MIMO DRA with complementary CP diversity. *IEEE Antennas Wirel. Propag. Lett.* **2021**, *20*, 1616–1620. [CrossRef]
10. Dwivedi, A.K.; Sharma, A.; Singh, A.K.; Singh, V. Circularly polarized two port MIMO cylindrical DRA for 5G applications. In Proceedings of the 2020 International Conference on UK-China Emerging Technologies (UCET), Glasgow, UK, 20–21 August 2020.
11. Patel, U.; Upadhyaya, T. Four-Port Dual-Band Multiple-Input Multiple-Output Dielectric Resonator Antenna for Sub-6 GHz 5G Communication Applications. *Micromachines* **2022**, *13*, 2022. [CrossRef]
12. Upadhyaya, T.; Park, I.; Pandey, R.; Patel, U.; Pandya, K.; Desai, A.; Pabari, J.; Byun, G.; Kosta, Y. Aperture-Fed Quad-Port Dual-Band Dielectric Resonator-MIMO Antenna for Sub-6 GHz 5G and WLAN Application. *Int. J. Antennas Propag.* **2022**, *2022*, 4136347. [CrossRef]
13. Girjashankar, P.R.; Upadhyaya, T.; Desai, A. Multiband hybrid MIMO DRA for Sub-6 GHz 5G and WiFi-6 applications. *Int. J. RF Microw. Comput.-Aided Eng.* **2022**, *32*, e23479. [CrossRef]
14. Alanazi, M.D.; Khamas, S.K. A Compact Dual Band MIMO Dielectric Resonator Antenna with Improved Performance for mm-Wave Applications. *Sensors* **2022**, *22*, 5056. [CrossRef]
15. Srivastava, K.; Dwivedi, A.K.; Sharma, A. Circularly polarized dielectric resonator-based multiple input multiple output antenna with pattern and polarization diversity for vehicular applications. *Int. J. Circuit Theory Appl.* **2021**, *49*, 3421–3433. [CrossRef]

16. Kulkarni, J.; Kulkarni, N.; Desai, A. A Two-Port Dual Band Microstrip Feed Based Cylindrical Dielectric Resonator Antenna Array for Sub-6 GHz 5G and Super Extended-C Band Applications. In Proceedings of the 2021 International Conference on Communication Information and Computing Technology (ICCICT), Mumbai, India, 25–27 June 2021.
17. Girjashankar, P.R.; Upadhyaya, T. Substrate integrated waveguide fed dual band quad-elements rectangular dielectric resonator MIMO antenna for millimeter wave 5G wireless communication systems. *AEU-Int. J. Electron. Commun.* **2021**, *137*, 153821. [CrossRef]
18. Mishra, S.; Das, S.; Pattnaik, S.S.; Kumar, S.; Kanaujia, B.K. Three-dimensional dual-band dielectric resonator antenna for wireless communication. *IEEE Access* **2020**, *8*, 71593–71604. [CrossRef]
19. Sun, Y.-X.; Leung, K.W. Substrate-Integrated Two-Port Dual-Frequency Antenna. *IEEE Trans. Antennas Propag.* **2016**, *64*, 3692–3697. [CrossRef]
20. Sharawi, M.S.; Podilchak, S.K.; Hussain, M.T.; Antar, Y.M. Dielectric resonator based MIMO antenna system enabling millimetre-wave mobile devices. *IET Microw. Antennas Propag.* **2017**, *11*, 287–293. [CrossRef]
21. Jadoon, A.; Sarfraz, H.; Owais, O.; Nasir, J. MIMO Dielectric Resonator Antenna Array for 5G Systems. In Proceedings of the 2022 19th International Bhurban Conference on Applied Sciences and Technology (IBCAST), Islamabad, Pakistan, 16–20 August 2022.
22. Varshney, G.; Gotra, S.; Chaturvedi, S.; Pandey, V.S.; Yaduvanshi, R.S. Compact four-port MIMO dielectric resonator antenna with pattern diversity. *IET Microw. Antennas Propag.* **2019**, *13*, 2193–2198. [CrossRef]
23. Sharma, A.; Sarkar, A.; Biswas, A.; Akhtar, M.J. A-shaped wideband dielectric resonator antenna for wireless communication systems and its MIMO implementation. *Int. J. RF Microw. Comput.-Aided Eng.* **2018**, *28*, e21402. [CrossRef]
24. Kavitha, M.; Shanthi, S.; Beno, A.; Arul Rajan, B.; Sathish, M. Design of 2× 2 MIMO-DRA antenna for 5g communication. *Int. J. Sci. Technol. Res.* **2020**, *9*, 7025–7029.
25. Hussain, M.T.; Sharawi, M.S.; Podilchack, S.; Antar, Y.M. Closely packed millimeter-wave MIMO antenna arrays with dielectric resonator elements. In Proceedings of the 2016 10th European Conference on Antennas and Propagation (EuCAP), Davos, Switzerland, 10–15 April 2016.
26. Hussain, M.T.; Hammi, O.; Sharawi, M.S.; Podilchak, S.K.; Antar, Y.M. A dielectric resonator based millimeter-wave MIMO antenna array for hand-held devices. In Proceedings of the 2015 IEEE International Symposium on Antennas and Propagation & USNC/URSI National Radio Science Meeting, Vancouver, BC, Canada, 19–24 July 2015.
27. Hussain, S.A.; Taher, F.; Alzaidi, M.S.; Hussain, I.; Ghoniem, R.M.; Sree, M.F.A.; Lalbakhsh, A. Wideband, High-Gain, and Compact Four-Port MIMO Antenna for Future 5G Devices Operating over Ka-Band Spectrum. *Appl. Sci.* **2023**, *13*, 4380. [CrossRef]
28. Das, G.; Sahu, N.K.; Gangwar, R.K. Dielectric resonator based multiport antenna system with multi-diversity and built-in decoupling mechanism. *AEU-Int. J. Electron. Commun.* **2020**, *119*, 153193. [CrossRef]
29. Kumari, T.; Das, G.; Gangwar, R.K. Spatially decoupled 8-port box shaped MIMO DRA with quad-directional pattern diversity. *J. Electromagn. Waves Appl.* **2021**, *35*, 1221–1234. [CrossRef]
30. Kiani, S.H.; Altaf, A.; Anjum, M.R.; Afridi, S.; Arain, Z.A.; Anwar, S.; Khan, S.; Alibakhshikenari, M.; Lalbakhsh, A.; Khan, M.A. MIMO antenna system for modern 5G handheld devices with healthcare and high rate delivery. *Sensors* **2021**, *21*, 7415. [CrossRef] [PubMed]
31. Sharma, A.; Sarkar, A.; Biswas, A.; Akhtar, M.J. Millimeter-Wave Quad-Port Multiple-Input Multiple-Output Dielectric Resonator Antenna Excited Differentially by TE 20 Mode Substrate Integrated Waveguide. In Proceedings of the 2019 URSI Asia-Pacific Radio Science Conference (AP-RASC), New Delhi, India, 9–15 March 2019.
32. Elfergani, I.; Rodriguez, J.; Iqbal, A.; Sajedin, M.; Zebiri, C.; AbdAlhameed, R.A. Compact millimeter-wave MIMO antenna for 5G applications. In Proceedings of the 2020 14th European Conference on Antennas and Propagation (EuCAP), Copenhagen, Denmark, 15–20 March 2020.
33. Sharma, A.; Sarkar, A.; Adhikary, M.; Biswas, A.; Akhtar, M. SIW fed MIMO DRA for future 5G applications. In Proceedings of the 2017 IEEE International Symposium on Antennas and Propagation & USNC/URSI National Radio Science Meeting, San Diego, CA, USA, 9–14 July 2017.
34. Dwivedi, A.K.; Sharma, A.; Singh, A.K.; Singh, V. Metamaterial inspired dielectric resonator MIMO antenna for isolation enhancement and linear to circular polarization of waves. *Measurement* **2021**, *182*, 109681. [CrossRef]
35. Chen, H.N.; Song, J.-M.; Park, J.-D. A compact circularly polarized MIMO dielectric resonator antenna over electromagnetic band-gap surface for 5G applications. *IEEE Access* **2019**, *7*, 140889–140898. [CrossRef]
36. Das, G.; Sharma, A.; Gangwar, R.K.; Sharawi, M.S. Performance improvement of multiband MIMO dielectric resonator antenna system with a partially reflecting surface. *IEEE Antennas Wirel. Propag. Lett.* **2019**, *18*, 2105–2109. [CrossRef]
37. Murthy, N. Improved isolation metamaterial inspired mm-Wave MIMO dielectric resonator antenna for 5G application. *Prog. Electromagn. Res. C* **2020**, *100*, 247–261. [CrossRef]
38. Karimian, R.; Kesavan, A.; Nedil, M.; Denidni, T.A. Low-mutual-coupling 60-GHz MIMO antenna system with frequency selective surface wall. *IEEE Antennas Wirel. Propag. Lett.* **2016**, *16*, 373–376. [CrossRef]
39. Dadgarpour, A.; Zarghooni, B.; Virdee, B.S.; Denidni, T.A.; Kishk, A.A. Mutual coupling reduction in dielectric resonator antennas using metasurface shield for 60-GHz MIMO systems. *IEEE Antennas Wirel. Propag. Lett.* **2016**, *16*, 477–480. [CrossRef]
40. Mabrouk, I.B.; E'qab, R.; Nedil, M.; Denidni, T.A. Hybrid isolator for mutual-coupling reduction in millimeter-wave MIMO antenna systems. *IEEE Access* **2019**, *7*, 58466–58474.

41. Farahani, M.; Pourahmadazar, J.; Akbari, M.; Nedil, M.; Sebak, A.R.; Denidni, T.A. Mutual coupling reduction in millimeter-wave MIMO antenna array using a metamaterial polarization-rotator wall. *IEEE Antennas Wirel. Propag. Lett.* **2017**, *16*, 2324–2327. [CrossRef]
42. Mu'Ath, J.; Denidni, T.A.; Sebak, A.R. Millimeter-wave compact EBG structure for mutual coupling reduction applications. *IEEE Trans. Antennas Propag.* **2014**, *63*, 823–828.
43. Tong, C.; Yang, N.; Leung, K.W.; Gu, P.; Chen, R. Port and Radiation Pattern Decoupling of Dielectric Resonator Antennas. *IEEE Trans. Antennas Propag.* **2022**, *70*, 7713–7726. [CrossRef]
44. Zhao, X.; Tong, C.; Yang, N.; Lu, K.; Wu, Z.; Long, Y. Radiation Pattern Decoupling of Low-Profile Substrate Integrated Dielectric Resonator Antennas. In Proceedings of the 2022 IEEE MTT-S International Wireless Symposium (IWS), Harbin, China, 12–15 August 2022; pp. 1–3.
45. Sahu, N.K.; Gangwar, R.K. Dual-Port Compact MIMO-DRAs: Exploiting Metallic Sheets to Increase Inter-Port Isolation at 28-GHz 5G-Band. *IEEE Trans. Circuits Syst. II Express Briefs* **2022**, *69*, 4814–4818. [CrossRef]
46. Liang, Y.-Z.; Chen, F.-C. Decoupling of Two Extremely Close Half-Volume Rectangular Dielectric Resonator Antennas. In Proceedings of the 2022 International Conference on Microwave and Millimeter Wave Technology (ICMMT), Harbin, China, 12–15 August 2022.
47. Elahi, M.; Altaf, A.; Almajali, E.; Yousaf, J. Mutual Coupling Reduction in Closely Spaced MIMO Dielectric Resonator Antenna in H-Plane Using Closed Metallic Loop. *IEEE Access* **2022**, *10*, 71576–71583. [CrossRef]
48. Wu, X.J.; Chen, Z.; Yuan, T.; Liu, S.Z. A Decoupling Method for E-Plane Coupled Millimeter-Wave MIMO Dielectric Resonator Antennas. In Proceedings of the 2021 Cross Strait Radio Science and Wireless Technology Conference (CSRSWTC), Shenzhen, China, 11–13 October 2021.
49. Yadav, M.; Sivadas, S.; Patel, P. Starfish-Shaped MIMO Dielectric Resonator Antenna. In Proceedings of the 2020 IEEE 17th India Council International Conference (INDICON), New Delhi, India, 10–13 December 2020.
50. Belazzoug, M.; Messaoudene, I.; Aidel, S.; Boualem, H.; Chaouche, Y.B.; Denidni, T.A. 4-port MIMO CDR Antenna based with a Defected Ground Structure for 5G mm-wave applications. In Proceedings of the 2020 IEEE International Symposium on Antennas and Propagation and North American Radio Science Meeting, Montreal, QC, Canada, 5–10 July 2020.
51. Abedian, M.; Khalily, M.; Xiao, P.; Kabiri, Y.; Tafazolli, R. Closely Spaced MIMO Dielectric Resonator Antenna for Sub 6 GHz Applications. In Proceedings of the 2022 International Symposium on Antennas and Propagation (ISAP), Sydney, Australia, 31 October–3 November 2022; pp. 237–238.
52. Zhang, Y.; Deng, J.-Y.; Li, M.-J.; Sun, D.; Guo, L.-X. A MIMO dielectric resonator antenna with improved isolation for 5G mm-wave applications. *IEEE Antennas Wirel. Propag. Lett.* **2019**, *18*, 747–751. [CrossRef]
53. Ali, A.; Tong, J.; Iqbal, J.; Illahi, U.; Rauf, A.; Rehman, S.U.; Ali, H.; Qadir, M.M.; Khan, M.A.; Ghoniem, R.M. Mutual Coupling Reduction through Defected Ground Structure in Circularly Polarized, Dielectric Resonator-Based MIMO Antennas for Sub-6 GHz 5G Applications. *Micromachines* **2022**, *13*, 1082. [CrossRef]
54. Kulkarni, J. Multi-Band Circularly Polarized Cylindrical Dielectric Resonator Multiple Input Multiple Output Antenna for 5G and X-Band Applications. In Proceedings of the 2021 IEEE Indian Conference on Antennas and Propagation (InCAP), Jaipur, Rajasthan, India, 13–16 December 2021.
55. Singhwal, S.S.; Kanaujia, B.K.; Singh, A.; Kishor, J.; Matekovits, L. Dual-band circularly polarized MIMO DRA for sub-6 GHz applications. *Int. J. RF Microw. Comput.-Aided Eng.* **2020**, *30*, e22350. [CrossRef]
56. Singhwal, S.; Kanaujia, B.; Singh, A.; Kishor, J.; Matekovits, L. Multiple input multiple output dielectric resonator antenna with circular polarized adaptability for 5G applications. *J. Electromagn. Waves Appl.* **2020**, *34*, 1180–1194. [CrossRef]
57. Song, S.; Chen, X.; Da, Y.; Kishk, A.A. Broadband Dielectric Resonator Antenna Array With Enhancement of Isolation and Front-to-Back Ratio for MIMO Application. *IEEE Antennas Wirel. Propag. Lett.* **2022**, *21*, 1487–1491. [CrossRef]
58. Li, R.-Y.; Jiao, Y.-C.; Zhang, Y.-X.; Wang, H.-Y.; Cui, C.-Y. A Wideband MIMO Triangular Dielectric Resonator Antenna with A Simple Decoupling Structure. In Proceedings of the 2020 9th Asia-Pacific Conference on Antennas and Propagation (APCAP), Xiamen, China, 4–7 August 2020.
59. Alanazi, M.D.; Khamas, S.K. On-Chip Multiband MIMO Dielectric Resonator Antenna for MillimeterWave Applications. In Proceedings of the 2021 30th Wireless and Optical Communications Conference (WOCC), Taipei, Taiwan, 7–8 October 2021; pp. 174–177.
60. Divya, G.; Babu, K.J.; Madhu, R. Quad-band hybrid DRA loaded MIMO antenna with DGS for isolation enhancement. *Int. J. Microw. Wirel. Technol.* **2022**, *14*, 247–256. [CrossRef]
61. Malhat, H.A.; Zainud-Deen, S.H. Low-profile quad-band perforated rectangular dielectric resonator antenna for wireless communications. *J. Eng.* **2017**, *2017*, 448–451. [CrossRef]
62. Vishwanath; Babu, R.; Sharma, V.; Sahana, B.C.; Varshney, G. Controlling the Resonant Modes/bandwidth using graphene strip and Isolation Enhancement in a Two-Port THz MIMO DRA. *Opt. Quantum Electron.* **2023**, *55*, 659. [CrossRef]
63. Li, M.; Cheung, S. Isolation enhancement for MIMO dielectric resonator antennas using dielectric superstrate. *IEEE Trans. Antennas Propag.* **2020**, *69*, 4154–4159. [CrossRef]
64. Pan, Y.M.; Qin, X.; Sun, Y.X.; Zheng, S.Y. A simple decoupling method for 5G millimeter-wave MIMO dielectric resonator antennas. *IEEE Trans. Antennas Propag.* **2019**, *67*, 2224–2234. [CrossRef]

65. Hagras, A.; Denidni, T.A.; Nedil, M.; Coulibaly, Y. Low-mutual coupling antenna array for millimeter-wave MIMO applications. In Proceedings of the 2012 IEEE International Symposium on Antennas and Propagation, Chicago, IL, USA, 8–14 July 2012.
66. Mishra, M.; Chaudhuri, S.; Kshetrimayum, R.S. Four-port DRA Array for MIMO Applications. In Proceedings of the 2020 International Symposium on Antennas and Propagation (ISAP), Osaka, Japan, 25–28 January 2021.
67. Sanghmitra; Rajput, A.; Mukherjee, B.; Patel, P. Y-shaped dielectric resonator MIMO antenna for omnidirection radiation pattern. *Electromagnetics* **2022**, *42*, 157–167. [CrossRef]
68. Iqbal, A.; Nasir, J.; Qureshi, M.B.; Khan, A.A.; Rehman, J.U.; Rahman, H.U.; Fayyaz, M.A.; Nawaz, R. A CPW fed quad-port MIMO DRA for sub-6 GHz 5G applications. *PLoS ONE* **2022**, *17*, e0268867. [CrossRef] [PubMed]
69. Anuar, S.U.; Jamaluddin, M.H.; Din, J.; Kamardin, K.; Dahri, M.H.; Idris, I.H. Triple band MIMO dielectric resonator antenna for LTE applications. *AEU-Int. J. Electron. Commun.* **2020**, *118*, 153172. [CrossRef]
70. Sharma, A.; Sarkar, A.; Biswas, A.; Jaleel Akhtar, M. Equilateral triangular dielectric resonator based co-radiator MIMO antennas with dual-polarisation. *IET Microw. Antennas Propag.* **2018**, *12*, 2161–2166. [CrossRef]
71. Abdullah, A.I.O.; Elshoshi, A.H.; Elmrabet, A.M.; Ahmed, S.M. Performance of Two-Port Dielectric Resonator Antenna Used for 5G mm-wave Applications. In Proceedings of the 2021 IEEE 1st International Maghreb Meeting of the Conference on Sciences and Techniques of Automatic Control and Computer Engineering MI-STA, Tripoli, Libya, 25–27 May 2021; pp. 782–786.
72. Pan, Y.M.; Hu, Y.; Zheng, S.Y. Design of low mutual coupling dielectric resonator antennas without using extra decoupling element. *IEEE Trans. Antennas Propag.* **2021**, *69*, 7377–7385. [CrossRef]
73. Lai, Q.X.; Pan, Y.M.; Zheng, S.Y. A Self-Decoupling Method for MIMO Linear and Planar Dielectric Resonator Antenna Arrays Based on Transmission Characteristics of Feeding Structure. *IEEE Trans. Antennas Propag.* **2023**, *71*, 5708–5716. [CrossRef]